Report

Micael C. Runnström

Is Northern China Winning the Battle against Desertification?

Satellite Remote Sensing as a Tool to Study Biomass Trends on the Ordos Plateau in Semiarid China

Ten-day intervals of satellite data between 1982 and 1993 are used to investigate the status of biological productivity on a rangeland in semiarid China exposed to high grazing pressure. Linear trends for 64 km^2 pixels are calculated through annual vegetation peak values, constructed by averaging the 6 Normalized Difference Vegetation Index (NDVI) values for August and September each year, and displayed in a GIS exposing the spatial and relative changes of biomass. Biological production, expressed as NDVI, has increased in general over the 12-year period and the correlation between precipitation and NDVI dynamic is tested. High increases are found for irrigated farmland along the Yellow River confirming a trend toward intensified cultivation and increased biomass from planted trees for farmland protection. Production on the rangeland has increased slightly without correspondence in rainfall. Instead, different measures implemented in the area to combat desertification are discussed as being likely explanations for the positive change.

INTRODUCTION

Pasture degradation has now reached critical levels in many pastoral areas in China (1) and the number of grazing livestock generally exceeds sustainable stocking levels.

In the 1950s, 1960s, and 1970s, many pastoral regions in semiarid China were subjected to sand encroachment and desertification (2, 3), the main cause being human-related activities, such as overgrazing, attempts to cultivate the fragile steppes, and collection of fuel wood and medical herbs. Today, rapid economic development and the growing population can, potentially, accelerate land degradation. In order to meet the increasing demand for food and to make up for the loss of arable land due to industrialization, urban expansion, extension of transportation links, etc., more marginal land is being transformed into farmland. The aim of a higher standard of living for the whole Chinese population will, according to Brown (4), increase the demand for more food variety. This will intensify use of arable land and the semiarid pasturelands, as the demand for more animal products increases. Increasing human impacts could accelerate erosion on the semiarid steppes of China and lead to decreasing productivity and a loss in arable and pastureland potential. In a global context, a decrease in biological production in the semiarid regions of China could affect world grain prices leading to negative impacts on many poor countries.

The aim of this study has been to investigate the trend of aboveground biomass as an indicator of land degradation status and land-use sustainability of a pastoral region in north central China. Twelve years of monthly images with 8 x 8-km pixel (picture element) resolution from the Advanced Very High Radiometer Resolution (AVHRR) sensor onboard the National Oceanographic and Atmospheric Administration (NOAA) satellites were analyzed over an area of almost 500 000 km^2. The seasonal behavior of green vegetation has been studied and the annual change between 1982 and 1993 was analyzed against precipitation.

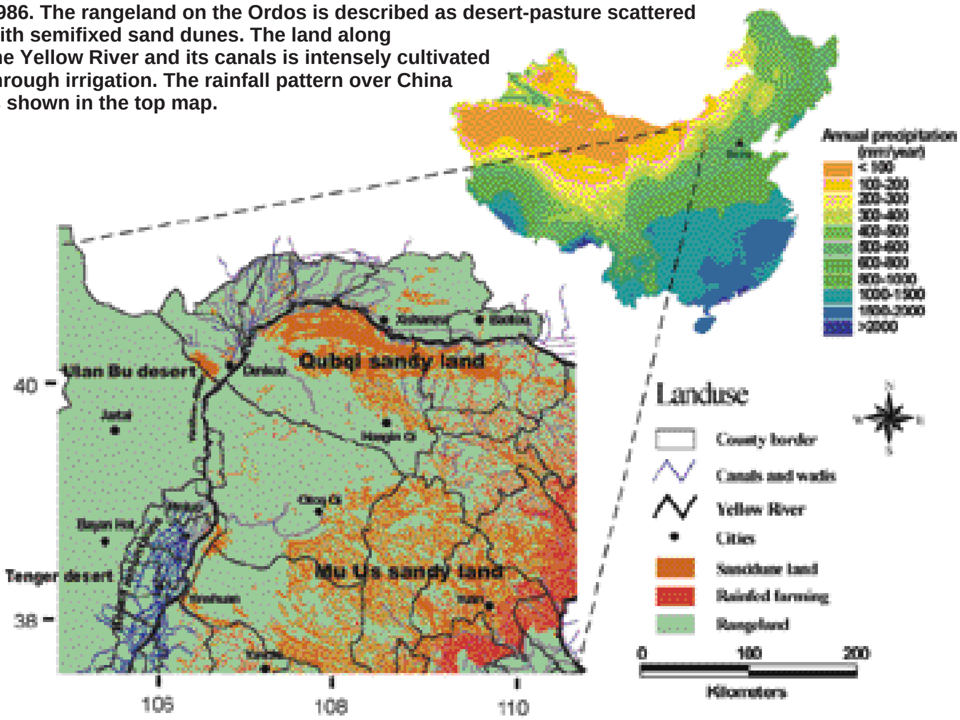

Figure 1. Landuse on the Ordos Plateau, interpreted from Landsat TM in 1986. The rangeland on the Ordos is described as desert-pasture scattered with semifixed sand dunes. The land along the Yellow River and its canals is intensely cultivated through irrigation. The rainfall pattern over China is shown in the top map.

THE STUDY AREA

The studied area (Fig. 1) is the Mu Us (Mauwushu) region on the Ordos Plateau that is administratively divided into the Shaanxi province, the Ningxia Hui Autonomous Region and the Inner Mongolia Autonomous Region (IMAR). The Ordos Plateau is often claimed to be among the most degraded pastoral areas in semiarid China (5, 6). The geographical coordinates are 37°–41°N/ 106°–111°E, and covers an area of approximately 120 000 km^2. The plateau has an elevation ranging between 1100 and 1600 m a.s.l.

As the Yellow River flows into the Loess Plateau, it veers northward and loops around the Ordos Plateau. Along the river, land has been cultivated for centuries and possibly millennia. At the start of the Ming Dynasty (1370 A.D.) there were already 4 major irrigation canals in the SW

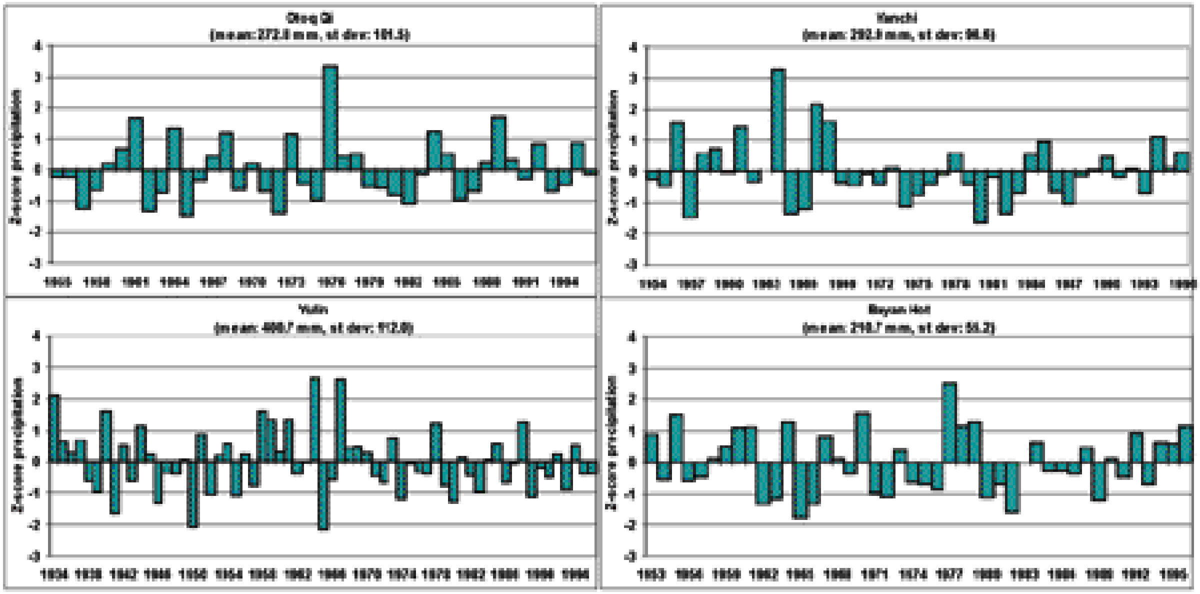

Figure 2. The standardized annual precipitation for 4 climate stations in the study area; Otoq Qi, Yanchi, Yulin, and Bayan Hot. The annual rainfall varies with 1–2 standard deviations. The geographical location of these climate stations is shown in Figure 9.

Figure 3. Population density (persons km^{-2}) of some Ordos counties from the Chinese Census in 1990. The ID-numbers are linked to county names and population change between 1982 and 1990 in Table 1.

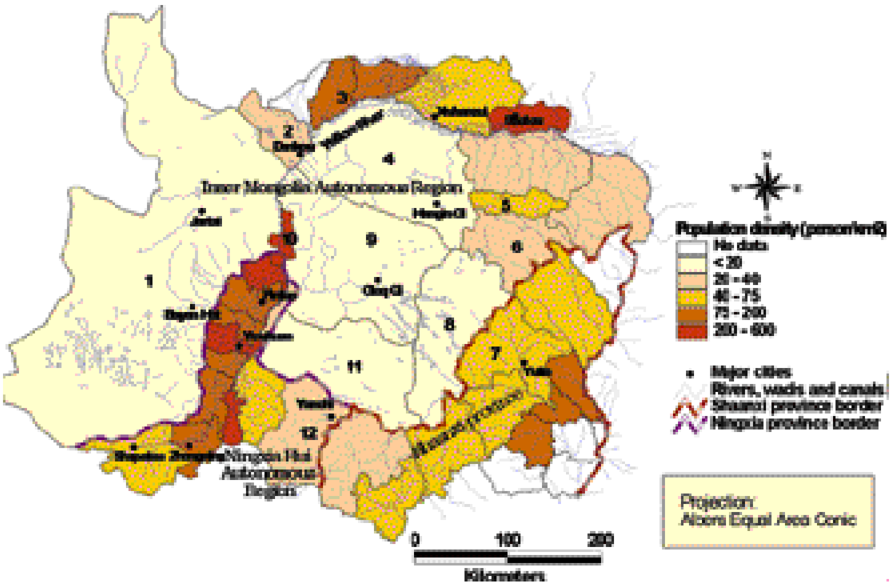

Table 1. The population density (persons km^{-2}) in the 1990 Chinese census and the population change in % between 1982 and 1990. The ID numbers are linked in Figure 3.

ID	County name	Population density 1990 (person km^2)	Population change (%) 1982–1990
1	Alashan-Zuo Qi	1.76	8.00
2	Dengkou Xian	32.57	8.40
3	Linhe Shi	179.39	21.30
4	Hangjin Qi	7.02	1.40
5	Dongsheng Shi	64.80	29.10
6	Yijinhuoluo Qi	23.29	7.90
7	Yulin Shi	53.12	23.50
8	Wushen Qi	8.11	11.10
9	Etuoke (Otoq) Qi	5.05	6.40
10	Wuhai Shi Shixia	383.44	22.10
11	Etuoke-Qian Qi	5.19	13.30
12	Yanchi Xian	21.23	16.20

corner of Ningxia and at the end of the Ming (about 350 years later) 38 000 ha of farmland were watered by canals (7). The irrigated fields and the Helan Mountains separate the plateau from the larger and more arid deserts in the west: the Tenger and Ulan Bu deserts. The Mu Us Sandy Land (in the south) covers an area of approximately 40 000 km^2, on the north edge of the Loess Plateau. In the north, the Qubqi Sandy Land extends over ca 15 000 km^2. Between these two sandy regions lies a vast rangeland, with a high potential of pasture degradation.

Climate

The climate is controlled by the Eurasian continental high- and low pressures, giving a cold, dry and windy climate from the northwest in the winter, while the summer is hot with moderate winds from the southeast bringing limited moisture into the area. Annual precipitation ranges from 400 mm in the southeast to 200 mm in the northwest. About 75% of the annual rains occur between June and September, the amount varying greatly between years. Through a calculated z-score, the annual deviation from the mean divided by the standard deviation, it appears normal for annual precipitation to fluctuate by 1 to 2 standard deviations from the mean (Fig. 2). In the more arid Tenger and Ulan Buh deserts in the west, annual precipitation is 150 mm. The seasonal variation in temperature shows a mean temperature of 22°C in July and –11°C in January for Otoq Qi. Climatologically, the Ordos Plateau lies in the temperate region, at the western edge of the monsoon zone in China. The Ordos Plateau is too dry for rainfed farming and almost all cropping is near river systems, where irrigation water is led to the cultivated plots through a system of canals. Evaporation in the growing season is high due to high temperature and frequent winds and, thus, traces of soil salinization and alkalization are observed in much of the Ordos.

Population

The current population density is rather uneven (Fig. 3) and the border between high and low density counties follows the boundary between China nonautonomous provinces and the IMAR, which in this region approximately coincides with the northern border of possible rainfed farming practices. The counties with population densities below 20 people km^{-2} are all located within the IMAR, where animal husbandry is exclusively practiced. In counties where cultivation is possible, the population is denser. This is on the margins of the Loess Plateau, in the south, where rainfed farming is practiced as well as the significant food producing counties along the Yellow River, where a dense web of canals draws river water for irrigation. Counties well endowed with natural resources, such as coal and oil are also more densely populated, i.e. Wuhai Shi have experienced rapid population growth between the censuses in 1982 and 1990 (Table 1).

The Pastures

The pastoral counties belong to the once famous Eerduosi Grasslands, and the Ordos fine wool breed of sheep is well known. The dominant grazing animal is sheep, but there are also a significant number of goats. The rangeland is classified as desert pasture and is characterized by 30–50% vegetation cover scattered with mobile and semifixed sand dunes. Nomadic Mongols have used these pastures for millennia, and according to historic records this area was in the first centuries A.D. '...a vast expanse of fertile land...' '...with plenty of water and fresh grass...' (8). At the beginning of the 5th century, Tongwan town, capital of the West Xia Dynasty, was built on what are today sandy areas, and historical records state that the natural environment at that time consisted of vast stretches of moist land with fresh water. Four hundred years later the sand dunes were as high as the town walls.

In the recent past, degradation of the Ordos pastures seems to have occurred in waves, related to periods of increased human activities. During the Great Leap Forward (1958–1960), the government urged farmers to extend cultivation into the rangeland and the Cultural Revolution (1966–1976) marked a second major attempt to intensify agriculture. Luk (9) concluded from satellite images and aerial photographs that the area covered by sand dunes increased between 1953 and 1976 and more intensely during 1959–1963 and 1971–1976. Despite a possibly shrinking area of pasture due to sand encroachment, the number of grazing animals in the IMAR has increased tenfold between 1947 and 1996 (10) (Fig. 4).

METHODOLOGY

The grasslands in China are not very productive. However, northern China supports the world's largest population of sheep and goats. The grasslands are overstocked and forage yield is below the required levels. This imbalance has caused degradation of the grasslands, reduction of biomass, decline of palatable species, and erosion (11). To investigate if land degradation processes or sand encroachment is occurring, the trend of biomass productivity from aboveground green vegetation between years was considered to be a viable indicator. Land degradation processes, either natural or human induced, would cause the vegetation cover to thin and the desert patches to increase in extent, and such changes may be monitored and measured using remotely sensed data, with a calculated vegetation index.

Multi-spectral satellite data can be linked to leaf area index, vegetation cover or biomass as the amount of absorbed radiation in the red part of the spectrum is related to the chlorophyll content of the plant, and the mesophyll structures and water content of the leaves control the reflection in the near infrared wavelengths. Ratios between these spectral bands are referred to as vegetation indices and the Normalized Difference Vegetation Index (NDVI) is a normalized ratio between the reflectances in the near infrared wavelength band (0.73–1.10 µm) and the red wavelength band (0.58–0.68 µm).

$$NDVI = \frac{NIR - \mathrm{Red}}{NIR + \mathrm{Red}} \qquad \text{Eq.1}$$

The normalization gives NDVI a potential range from between –1 and +1, and active green vegetation gives the index a positive value. The NDVI is the most widely used vegetation index and numerous studies have demonstrated its ability to describe vegetation phenology (12, 13) and indicate environmental conditions (14). Reviews of applications with the NDVI are given in Ehrlich et al. (15) and Eklundh (16).

Calculating a biophysical property like Net Primary Production (NPP) from NDVI requires an input of Photosynthetic Active Radiation (PAR), i.e. the amount that depends on latitude, time of year and cloudiness. Additionally, a value of the efficiency of the ecosystem to convert light to organic matter is needed for NPP modelling. Quantitative determination of NPP has not been the objective of this study due to lack of field measurements to evaluate against. However, relative changes of biomass production, expressed as NDVI in time and space, do provide essential information of land degradation status through vegetative change. A relative change of NDVI can be related to a corresponding theoretical change of annual precipitation, which is interesting, as rainfall is the most limiting variable for vegetative production in semiarid environments.

An intricacy using biomass to measure productivity change is that vegetation in semiarid regions is responding to the annual rains and, just like rainfall, fluctuates between years and also temporally during the vegetative season (Fig. 5). Measuring trends of produced biomass thus requires a multi-annual data set with repetitive images taken sequentially in each annual vegetative period. It is then possible to calculate a seasonal value to base the trend on and to compare it to the corresponding trend in rainfall. Studies on vegetative change in drylands using remotely sensed data have previously only been possible by comparing 'snapshot' images taken in different years. The timing of acquisition of these images is, due to the annual phenology of vegetation in response to, primarily, precipitation, consequently, critical as the amount and time of rainfall varies between years. Moreover, the availability of images is also limited and this makes it difficult to obtain a comparison of even the same month between years. This is likely to be a source of error and uncertainty in many previous desertification-rate studies. The development of multi-annual data sets with high temporal resolution has therefore been requested for more reliable change detection studies. The NOAA Pathfinder data set is available with a spatial resolution of 8 x 8 km^2 at temporal resolution of 10-day interval maximum composites, equalling 36 images annually. At present, the time series is complete between 1982–1993, and this has been used in this study. The phenology and dynamics of vegetation can then be studied at 10-day intervals. In the study area, the annual NDVI maximum occurs in August–September, at the end of the rainy period (Fig. 6). In each 64 km^2 pixel, the 10-day values were used to calculate a vegetation peak (VP) seasonal value as the average of the 6 NDVI-values in August and September. A VP-value should be better comparable between years to produce a trend, as the timing of the annual rains would not influence the NDVI comparison and the correlation between

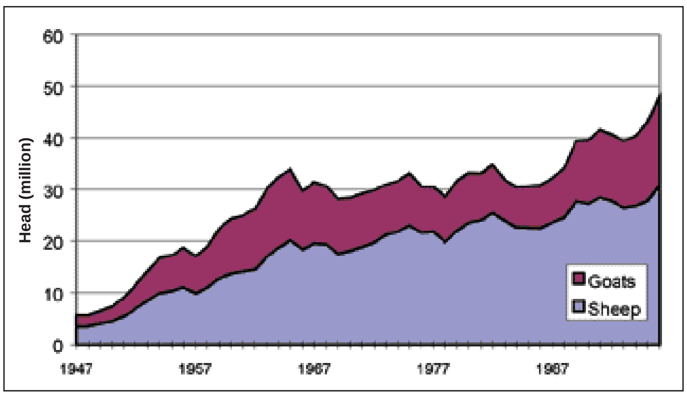

Figure 4. The total number and partition of sheep and goats in the IMAR between 1947 and 1996. Source: Statistical Yearbook of Inner Mongolia 1997, Hohot (10).

the amount of summer rain and the VP-value can be analyzed. Calculating an averaged annual VP-value would also filter out extreme values caused by clouds, aerosols, etc. and a trend should show a more significant direction. The same 64-km^2 pixel is analyzed through the time series and spatial differences, e.g. varying soil conditions, is not affecting the trend at pixel level. An averaged spring season NDVI value was also calculated by averaging the nine NDVI values in March, April, and May to compare the amount of biomass at the end of the dry season between years. However, spring measurements are more uncertain, as vegetation is so scarce that reflection from the soil dominates the measured radiation.

THE NOAA AVHRR PATHFINDER DATA SET

The National Aeronautics and Space Administration (NASA) and NOAA through the Earth Observing System (EOS) Program Office jointly created the NOAA AVHRR Land Pathfinder program. The aim was to design a long-term multi-channel global data set with stable calibration to be suitable for global change, climate research studies. The high temporal resolution and the long time series of the data set makes it an improved tool for monitoring terrestrial environments and studies of vegetation dynamics. Apart from measured reflectance in the red and the near-infrared wavelength bands the Pathfinder data set also contain calculated NDVI-values.

Pre-processing at NASA

The principal perturbations that affect radiation on its way through the atmosphere are differential molecular and aerosol scattering, ozone, and water vapor (17). The radiometric corrections executed on the NOAA Pathfinder data set include corrections for Rayleigh scattering, ozone absorption and optical thickness and the resulting reflectances have then been normalized for incoming solar illumination (18). The amount of atmospheric aerosol and water vapor vary highly in time and space, but due to lack of ancillary data sets for these concentrations no corrections for water vapor and aerosols have been performed. Calibration errors concerning solar-zenith-angle normalization, Rayleigh scattering and ozone absorption have been noticed for the data set, but the calibrations executed in the pre-processing are to date still the best available.

Evaluating the Stability of the NOAA Pathfinder Data Set

The NOAA Pathfinder data set has been pre-processed and calibrated at NASA to be available as a ready-to-use operational data set. However, the stability and reliability of the data set depends on whether sufficient intersatellite calibrations have been applied that can compensate for the differences in sensor performance between the satellites. Time also affects the sensors onboard the NOAA satellites, as the sensitivity to measure radiation decreases over time and is referred to as "sensor degradation". Additionally, the NOAA satellites encounter a slight orbital drift that changes the local passing time throughout the operational lifetime and the measured reflection from the terrestrial surface is thus modified due to a change in the incident solar angle.

To evaluate the stability of the NOAA Pathfinder data set, a window containing mobile sand dunes without vegetation—visited during fieldwork in September 1995—was chosen north of Jartai in the Ulan Buh Desert (Eval-site in Fig. 9). A nonvegetated site was preferred, as changes in the measured signal caused by inaccurate corrections would otherwise be overshadowed by the dynamic of vegetative growth and status. The NDVI values are low (0.0) and decreasing when the rain period starts confirming a nonvegetated location, as more of the near-infrared wavelengths are being absorbed by the increase in moisture than are the red wavelengths. NDVI is therefore decreasing as opposed to a vegetated site that encounters increase in NDVI as the rain is used for increased photosynthetic activity. A climate station is located just outside the window, measuring an annual precipitation of 109 mm with a 46 mm standard deviation.

As the data set contains data from 3 different NOAA satellites (NOAA-7, NOAA-9 and NOAA-11), a consistent calibration of the data to correct for intersatellite shifts through the 12

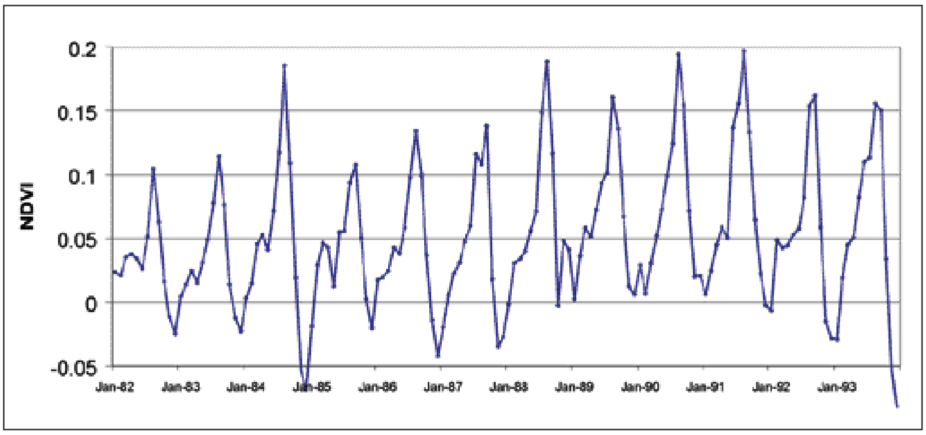

Figure 5. Monthly NDVI values between 1982 and 1993 for a 576 km^2 window outside Otoq Qi. The graph shows the annual and seasonal variations for biological production expressed through NDVI. The site represents semiarid pasture steppe.

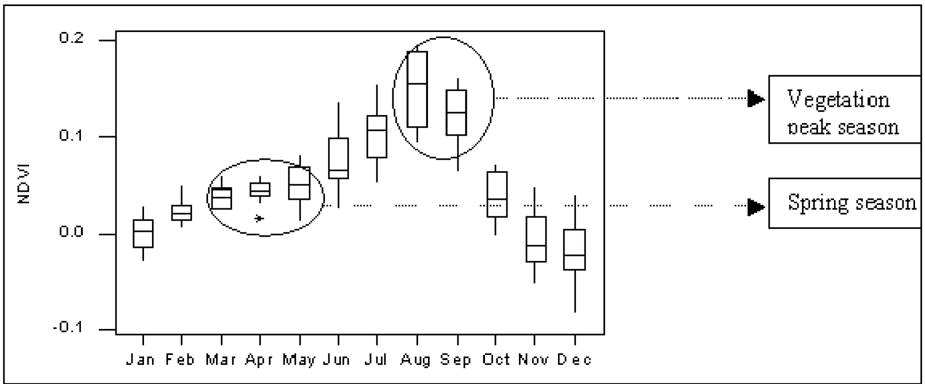

Figure 6. A box plot showing the annual NDVI dynamic or vegetation phenology expressed as monthly mean values between 1982 and 1993. The box plot shows the median, the first and third quartiles, the max and min values and the outliers (asterisk). The Vegetation Peak season is calculated as the mean value of the August and September NDVI values. The Spring season is the mean value calculated from the 3 months: March, April and May.

years of data is essential, to form a stable and reliable data set. This has been possible by viewing bright targets such as deserts, high clouds, etc., but Myneni et al. (19) found increasing anomalies in the global AVHRR NDVI data set that corresponded in time to the change in satellites from NOAA-9 → NOAA-11. The operational periods of image registration within the Pathfinder data set for each of the satellites are listed in Table 2.

The annual dynamic range of NDVI for the evaluation site is quite moderate compared to a vegetated site, and the existing variation and dynamic range is probably linked to differences in soil and atmosphere humidity, and a varying presence of aerosols. As water significantly absorbs the near infrared radiation, the main cause of variation is probably changes in water content at the surface or in the atmosphere.

The annual NDVI variance was analyzed in order to test if the years corresponding to the launch of new satellites (1985 and 1988) showed significant variance anomalies, but only the years 1984 and 1993 differed from normal. The high variance in 1984 can probably be explained by a corresponding high variance in annual precipitation for 1984 (no precipitation data for this site were available for 1993). To further analyze the intersatellite shifts, NDVI deviations between the months after and before a satellite shift were compared over the 12 years. The years 1985 and 1988 do show anomalies for the corresponding periods that may indicate that the calibration of data between satellites is not efficient. Both satellite shifts occur in the dry season and the NDVI differences are smaller than the yearly amplitude and, hence, may not have a significant effect on the annual dynamic range and stability.

NDVI anomalies through the time series were analyzed to evaluate whether sensor degradation is affecting the data set, hypothesiszing that monthly anomalies are likely to show a trend with time if corrections were inadequate. The trend for the monthly anomalies through the complete time series was found to be slightly positive. When splitting the monthly anomalies into time periods that correspond to the 3 satellites, the trends for NOAA-7 and NOAA-11 are close to zero. The NOAA-9 period on the other hand, shows a strong negative trend that cannot be explained by any corresponding monthly precipitation anomalies. This could indicate that the corrections for sensor degradation of the Pathfinder data set might not be appropriate for the NOAA-9 time period.

As the dominating anomalies occur in the dry season and the objective of this study is to assess relative changes of biological activity, the evaluation-site was compared to 2 vegetated rangeland sites, to evaluate if any intrinsic trend of NDVI for the vegetation peak season exists in the data set. The non-vegetated site showed a trend very close to zero between 1982 and 1993, as opposed to the vegetated sites that experienced a trend towards increasing NDVI (Fig. 7).

The Pathfinder data set is, according to the tests described above to evaluate intersatellite shifts and sensor degradation, regarded as reasonably stable and thus reliable with a modest intrinsic positive trend in NDVI when comparing the vegetation peak value over the complete time series. The introduction of data from different satellite sensors is discernible in the data set on a monthly time scale, but does not seem to affect the yearly time-scale dynamic. Lack of precise correction algorithms for sensor degradation seems obvious for the NOAA-9 period, and the negative trend of NDVI cannot be explained by any corresponding precipitation trend. Furthermore, using this time period only may be questionable.

TRENDS OF BIOLOGICAL PRODUCTIVITY

A scatter plot was produced between mean annual precipitation for the 6 climate-stations used in this study and the corresponding averaged VP-NDVI between 1982 and 1993 (Fig. 8). Average VP-NDVI expressing density of vegetation cover or biological productivity was found to be related to annual precipitation in an almost perfect correlation ($R^2 = 0.95$, $P < 0.001$, $n = 6$). A change in NDVI can thus, theoretically, be expressed as corresponding change in annual rainfall through the linear equation: $y = 1388.6 \cdot NDVI + 114.5$, where y is the annual rainfall.

For VP-NDVI the slope of the linear trend of best fit through the 12 years in each 64 km^2 pixel was calculated using the least square method. A negative regression coefficient suggests a decline of bio-productivity and a positive regression coefficient suggests an increase. NDVI trend data were extracted for a 24 000 km^2 large area in the center of the Ordos, representing semiarid steppe rangeland. The study shows that for the spring season, the average pixel would, if the trend is followed, increase by 0.014 NDVI units over the 12 years. In the vegetation peak season, the average pixel increases with 0.05 NDVI units, which would equal a theoretical increase of 69 mm rainfall or ca 25% increase, taking Otoq Qi as an example. For the irrigated and intensely cultivated regions along the Yellow River, NDVI values for an area equalling 8640 km^2 were extracted and the average pixel increased by 0.09 NDVI units for the vegetation peak season.

Table 2. The time periods of registering data within the NOAA Pathfinder data set for each of the 3 succeeding satellites.

Satellite	First date	Last date
NOAA 7	2 May 1981	24 Feb 1985
NOAA 9	25 Feb 1985	8 Nov 1988
NOAA 11	9 Nov 1988	31 Dec 1993

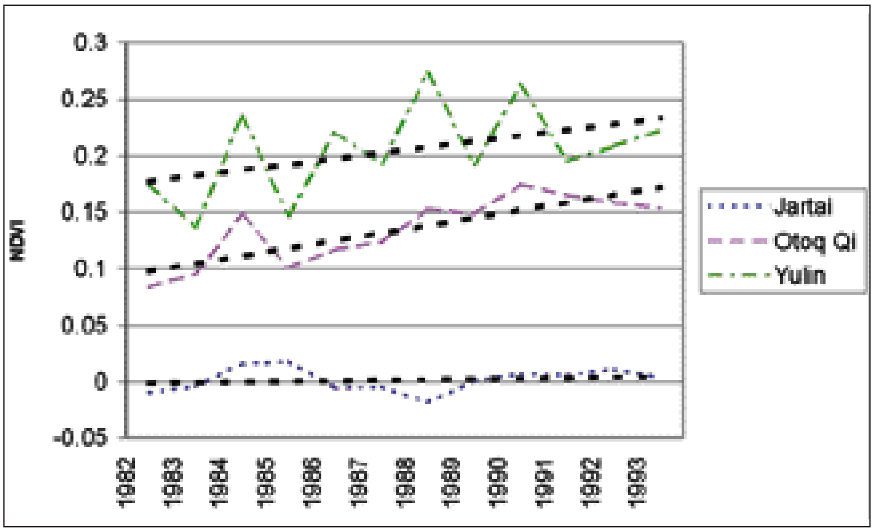

Figure 7. A comparison of vegetation peak season NDVI values and linear trends between the nonvegetated evaluation site (Jartai), a ~ 30% vegetated site (Otoq Qi) and a ~ 50% vegetated site (Yulin).

The gain coefficient values were re-classed into 5 classes that describe the NDVI change over the 12 years as derived from the linear trends:

– High increase: > 0.1 NDVI units over the 12 years.
– Slight increase: Between 0.03 and 0.1 NDVI units.
– No change: ± 0.03 NDVI units.
– Slight decrease: Between –0.03 and –0.1 NDVI units.
– High decrease: > –0.1 NDVI units.

These were then graphically mapped in a Geographic Information System (GIS) revealing the spatial distribution and relative change of biological productivity, as expressed through NDVI (Fig. 9). To evaluate the correlation between NDVI and rainfall and the significance of the linear trends, 8 windows of 576 km^2 (3 x 3 pixels) each were extracted. These were chosen in the vicinity of climate stations as well as highly sensitive areas experiencing significantly positive or negative trends. Five climate stations were used to evaluate the influence of variations in rainfall and response in NDVI. The correlation was calculated between VP-NDVI and summer precipitation for the 12 years to determine if and how the interannual variation of rainfall was linked to the measured changes of NDVI.

The extracted windows represent:
– Area 1: A 'no change' arid pasture site.
– Areas 2–5: Small increase of NDVI on pastureland.
– Areas 6–7: Sites with a high decrease of NDVI.
– Area 8: High increase of NDVI in irrigated areas.

A window west of Bayan Hot was analyzed (Area 1) on the margin of the Tenger Desert (100 km south of the evaluation site Jartai). The land use is solely pastureland for sheep and goats with a corresponding vegetation cover of 10–30% as of 1995. Bayan Hot receives a mean annual rainfall of 210 mm. VP-NDVI and the summed precipitation for July, August and September are well correlated at this site over the 12 years with $R^2 = 0.84$ ($P < 0.001$; $n = 12$) and presumably precipitation is the dominating variable responsible for the measured NDVI fluctuations. Between 1982 and 1993, the trend was close to zero for both NDVI and rainfall (Fig. 10).

Windows representing pastureland steppes on the Ordos Plateau with a slight increase in NDVI, all have lower correlations with rainfall. Zhongning (Area 2): $R^2 = 0.47$ (P = N.S. (0.688); $n = 12$), Yanchi (Area 3): $R^2 = 0.26$ ($P < 0.01$; $n = 12$), Otoq Qi (Area 4): $R^2 = 0.35$ ($P < 0.05$; $n = 12$) and Yulin (Area 5): $R^2 = 0.38$ ($P < 0.05$; $n = 12$). Three of four sites have rainfall trends close to zero for the corresponding time period and only Otoq Qi has measured increasing rainfall. This implies that the registered increase of biological activity is not a result of more rainfall over the time period. According to the linear trend for Yanchi

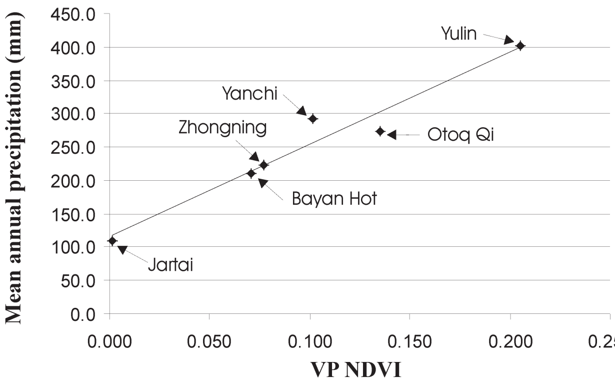

Figure 8. A linear relationship seems obvious between mean annual rainfall and averaged VP-NDVI for the 6 climate stations and a higher annual precipitation thus equals higher biomass productivity. The increase in NDVI as derived through a linear trend at a site can thus be related to a theoretical increase of rainfall using the formula $y = 1388.6 \cdot NDVI + 114.5$.

Figure 9. The linear trends of the vegetation peak season NDVI between 1982 and 1993 for each 64 km^2 pixel. The gain coefficients of the slopes were re-classed into 5 classes ranging from high increase to high decrease of NDVI. The corresponding range of NDVI for each class is described in the text.

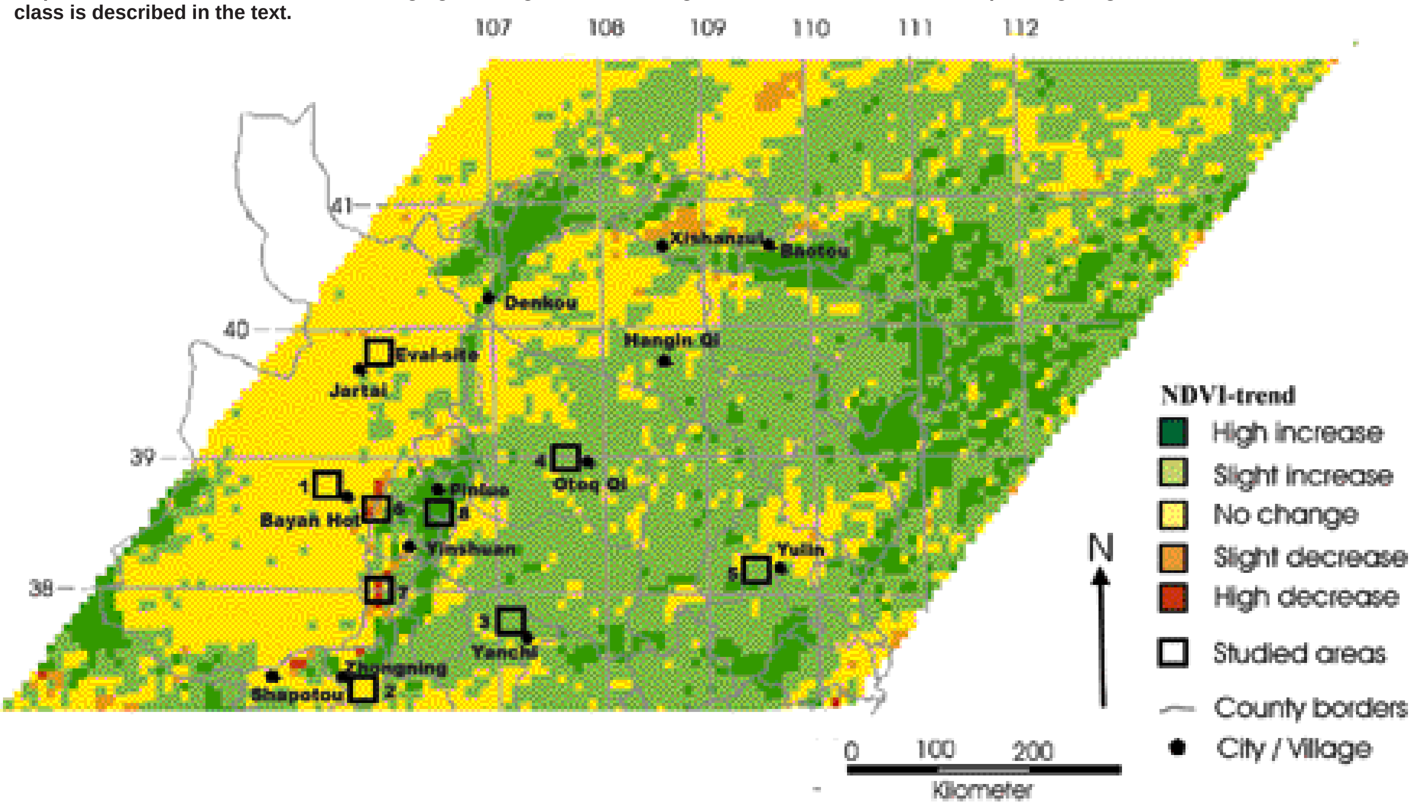

(Area 3), NDVI has increased 0.05 units over the 12 years, which according to equation 2, equals an extra 68 mm of average yearly rainfall, from 293 to 361 mm, a 23% increase. For Yulin (Area 5), receiving an average of 400 mm annually, the increase of NDVI units corresponds to an extra 21% of mean yearly rainfall. For Otoq Qi (Area 4) the theoretical increase of rainfall corresponds to 111 mm or 41%, but at this site the rainfall trend is positive and has, according to the linear trend, increased by 54 mm, which is approximately half of the NDVI increase. Hence, increased NDVI values at all these 3 rangeland sites correspond to a theoretical increase in mean yearly precipitation of about 20%.

Few sites in the study area indicate decreased biomass through a negative linear trend of NDVI. The trend for Area 6 and Area 7 implies that the vegetation cover may have been reduced over the time period. Area 6 is located in the Helan Mountains, separating the Ordos rangeland from the Tenger Desert. The vegetation is dominated by planted spruces (*Pinus sylvestris* var. *mongolica* and *P. tabulaeformis*) that are being pruned for fuelwood collection (according to information from local residents in 1997). The trend may be assessed by visual examination and by inspecting the P-value (0.181), the negative trend is not statistically significant. On the other hand, the NDVI values for the spring season (March–May) indicate a more regular decline at this site. The site shows a fair correlation with precipitation ($R^2 = 0.40$) although the rainfall was measured at the Bayan Hot climate station, west of the site at the foot of the mountain. The abrupt change, as seen in Area 7, is probably the result of human activities. This site was visited during fieldwork in 1999, but instead of finding an area with reduced vegetation cover, the site today consists of planted protective farmland forest. The decrease of NDVI sensed by the NOAA satellite in the late 1980s is probably related to soil preparations before the planting took place and the vegetative growth of poplars, grapevines and pears was not registered as it occurred after 1993 and thus is not included in the time series. Today, irrigation water for the vegetation is directed from the Yellow River.

The irrigated and intensely cultivated areas along the Yellow River show strong positive NDVI trends between 1982 and 1993 (Area 8). This is most likely a combined effect of increased use of fertilizers and expansion of the cultivated land area, but also increased biomass from planted trees for farmland protection. No climate station was available to correlate precipitation data with NDVI, but biomass productivity here is less dependent on precipitation, because of irrigation.

An east-west difference is apparent when comparing standardized trends in NDVI and precipitation (Fig. 11). The NDVI trends for the eastern sites have stronger positive direction and differ more from the rainfall trends than the sites in the drier west. This could imply that the biological production in the east of the study area has not increased as a result of more rainfall, and explanations should perhaps be sought in changes in human activities, management, and land use. The low correlation between rainfall and NDVI at the eastern sites would confirm such an explanation for the increase in biomass. Otoq Qi experienced the most positive standardized trend in NDVI, but is also the only site with a positive rainfall trend.

CONCLUSION

The simple method to calculate linear trends through the available time series of NOAA AVHRR NDVI data described in this

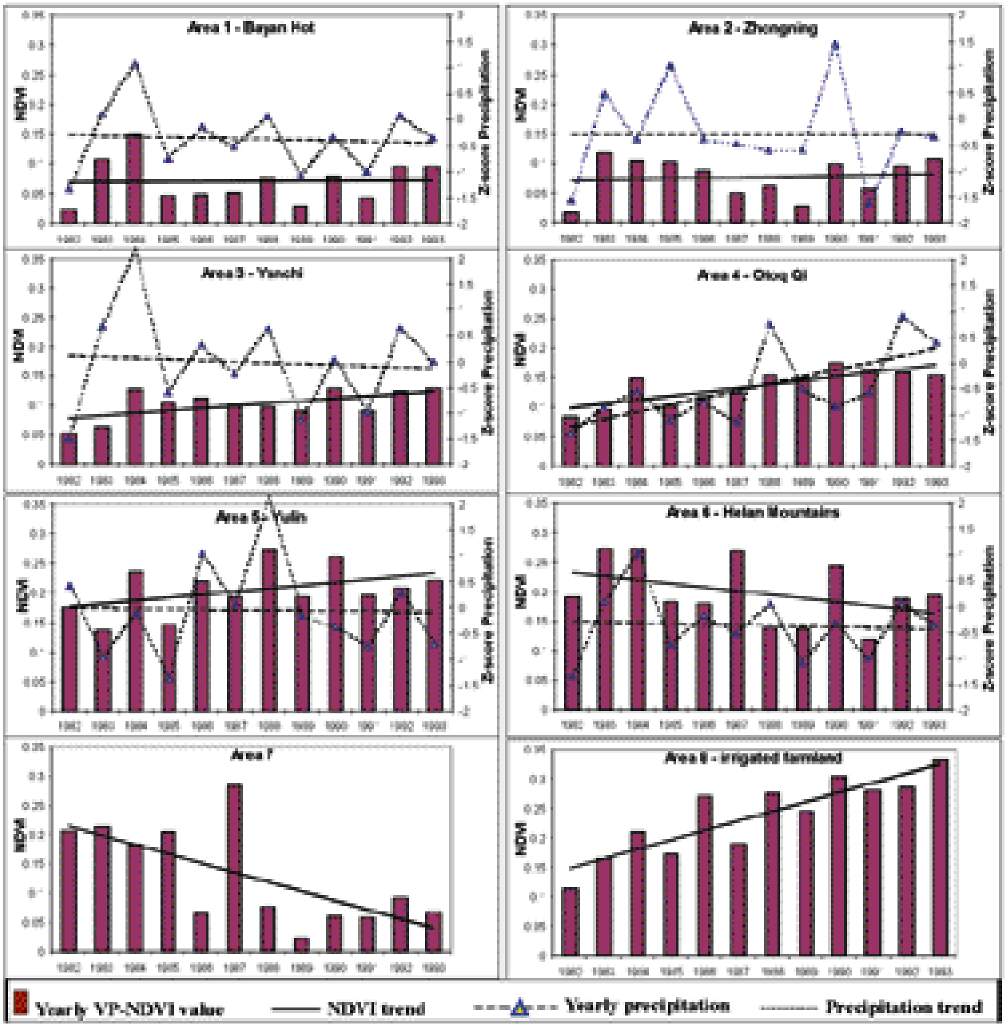

Figure 10. The annual VP-NDVI and precipitation over the 12 years studied for the 8 extracted 576 km^2 windows (Area 1–8). Each window consists of 9 pixels and an average NDVI-value was calculated. Linear trends have been calculated through VP-NDVI and rainfall. For statistics and site descriptions see text.

paper proves to be a fast, convenient and comprehensive way to obtain a spatial overview of vegetative change at the regional scale. It must be stressed that NDVI is not equal to green biomass, but many studies have shown a high correlation between NDVI and percentage vegetation cover (R^2 = 0.86 on grasslands in Mongolia) (20).

An interesting spatial pattern is revealed for the map displaying the gain coefficients for NDVI trends between 1982 and 1993 (Fig. 9). The distribution of pixels with high positive trends follow the Yellow River and its irrigation canal system very precisely. This could be expected, as the biological productivity due to increased use of fertilizers and the spatial extent of irrigated areas is believed to have increased over the 12 years studied, resulting from China's effort to increase production from the agricultural sector. It was also expected that pixels covering the more arid deserts in the west would show a 'no change' behavior regarding the amount of biomass. However, it is surprising that the rangeland of the Ordos indicates slight increased bio-productivity, even though both human and animal populations have increased in this area over the 12-year period.

Five climate stations distributed along a rainfall gradient were used to evaluate the influence of variations in rainfall and response in NDVI by comparing the coefficient of determination, R^2, between summer rain and vegetation peak NDVI. The correlation was found to be higher in the more arid west, i.e. Bayan Hot, R^2 = 0.84 compared to Yulin in the east with R^2 = 0.38. This would indicate that in the arid west the amount of rainfall is dominating the response in biological productivity. However, in the east, some other variable seems to be causing increased biological productivity. Four of the 5 climate stations show trends close to zero for precipitation and the positive biomass trends could be the result of desertification control measures implemented in the area over the last 40 years. The NOAA Pathfinder data set does seem to have a slight intrinsic positive trend due to insufficient calibrations, but the positive trends exhibited in the rangeland are notably greater.

DISCUSSION

The results shown in this study could imply that the extensive land reclamation activities throughout China that are hoped to reverse decades of environmental misuse are beginning to pay off. Already in 1955, the Chinese Government decided to plant shelterbelts for sand stabilization in the semiarid regions. In 1978, the government approved *The Three-North Project* or *The Green Great Wall*, a massive shelterbelt-system designed to obstruct advancing sand encroachment in the northern provinces. The system is composed of trees and shrubs and between 1978–1985 around 5 mill. ha were planted (21). In a second stage, completed in 1995, a total of about 8 mill. ha have been afforested. It is difficult to quantify the additional biomass added from these projects, as the survival rate for planted trees and seeds are generally poor in the semiarid regions. A survey made by the Northwest Institute of Forestry in Xiían, Shaanxi, indicated that half of the reported national afforestation claims were false, and that the survival rate of planted trees was only 40% (22). However, more positive descriptions of the afforestation projects have been reported elsewhere (23, 24).

Figure 11. A comparison of the linear trends for precipitation and corresponding NDVI at 5 sites. The trends have been standardized by calculating annual Z-scores as the deviation from the mean divided by the standard deviation for the 12 years in the time series. A linear trend was then calculated through the Z-scores. This makes all trends for both NDVI and rainfall comparable. At each location the deterministic coefficient (R^2) for the correlation between rainfall and NDVI-dynamic is given. The sites are ordered in west–east positions which also describe the gradient of mean annual rainfall from 210 mm for Bayan Hot to 400 mm for Yulin.

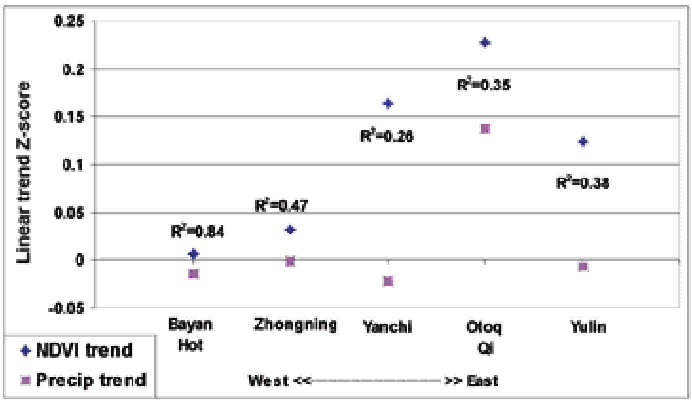

Parts of the Ordos pasturelands were aerially seeded in the 1980s and 1990s, to increase the steppe vegetation and to stabilize sandy soils. This measure is rather new, but has proven successful in regions where annual rainfall exceeds 400 mm. Areas on the Ordos where aerial seeding has been successful are around Yulin, where precipitation is sufficient. Areas with less rain have also been seeded from aeroplanes but with mixed results. The regions south of Otoq Qi have been aerially seeded with good results (statements from Otoq Qi climate station with an annual precipitation of 275 mm). As shown in this study, the area between Yulin and Otoq Qi does exhibit positive trends of NDVI. However, the areas west and south of Bayan Hot, receiving only 210 mm rain annually, show poor germination. Between 1981 and 1991, a total area of 872 km^2 was aerially seeded and in 1985 alone (a drier year than average) 340 km^2 were seeded (data from Bayan Hot climate station). According to this study, no sign of improving vegetation is yet visible in this area. The progress of aerial seeding is of course very sensitive to the timing of the rains and can probably be a good measure to increase biomass in semiarid regions if sowing coincides with moist years.

The introduction of the Household Production Responsibility System (HPRS) in rural areas in the mid-1980s may also have contributed to increased biomass. This reform—to contract-out rangeland to households—was intended to increase fenced areas protected from overgrazing. In addition the contractors are called on to plant trees on their land. Ho (25) is critical of the environmental benefits from the HPRS, owing to the difficulties in implementing and enforcing rangeland policies. Ho considers, from studies in Yanchi county, that fencing has failed and the pastoral farmers still use officially protected rangeland.

Very few areas indicate a decline in NDVI and some of these can possibly be related to human exploitation. The area is rich in coal, oil, and natural gas and expanding mining areas could lead to declining vegetation. On the other hand, the pressure might ease on surrounding rangeland as former pastorals earn more money working in mining industries.

Some sites have shown that the trends are not statistically significant. This is of course a drawback in the generalization used in this study. A linear trend can hardly describe the complex dynamics of an environmental feature, such as biological production. Higher degree polynomials would better fit the NDVI data series, but this is risky as they are not stable and would be difficult to display graphically.

For some areas, a few of the years prior to 1982 had below average rainfall that may have affected regeneration of the vegetation and consequently lowered vegetation cover. Moreover, a low initial NDVI value at the beginning of the time series could result in a higher gain coefficient than might actually be the case if climatic conditions are normalized later in the time series. The pixels corresponding to negative trends would then probably be underestimated. Nevertheless, the trend differences between rainfall and NDVI, shown in the results, implies that biomass on the eastern side of the Ordos Plateau has increased without a corresponding gain in rainfall. The annual differences in rainfall makes change studies in semiarid environments, using vegetation as indicator, precarious. Longer time series than the 12 years used in this study, are preferable. A normal period for climate data is usually 30 years and would be a satisfying time series for change studies. The NOAA Pathfinder data set is nevertheless the longest available that has a temporal resolution convenient for vegetation monitoring and the intention of NOAA/NASA is to extend the available data series in the near future. To get an overview picture of biomass change in a region, it might still be wise to use 12 years of high temporal resolution satellite data, compared to the otherwise available 'snapshot'-image comparison, the relationship between biomass dynamic and variations in precipitation can then be analyzed. If the aim, on the other hand, is to monitor local small-scale changes, then high geometric resolution satellite images will still be more suitable to use in combination with soil fertility measurements. However, this latter is more costly.

The coarse resolution of the NOAA pathfinder data set is a condition to reduce the amount of data that otherwise would be almost impossible to handle for such long time series. A maximum composite sampling technique is used to extend the pixel resolution from the satellite-registered ~1 km^2 via 16 km^2 to 64 km^2. The value of the daily 16 km^2 global area coverage (GAC) pixel with highest NDVI during each 10-day interval is given to the geographically corresponding 64 km^2 pixel. This composite technique reduces the risk of clouds and other unwanted atmospheric perturbations entering the data set. The NDVI value of each 64 km^2 composite pixel through the time series might therefore represent reflection from different parts within the pixel. But as the highest NDVI value always is chosen it is most likely the same part, unless clouds are covering the most vegetated part every satellite crossing during the 10 days. Due to the composite technique and resampling to 64 km^2 pixels, it is possible for a part of the pixel to undergo a vegetation decline as long as the part containing the highest photosynthetic activity is kept unchanged. This is of course a drawback with a data set constructed like the NOAA Pathfinder data set. The composite technique used makes it very uncertain for calculating physical properties like kg ha^{-1} of biomass in relation to registered NDVI values or trends. The intention of this study has only been to investigate the spatial pattern and relative trends of biological production and to relate these to actual precipitation and the results make it easier to select interesting regions for further exploration using other techniques.

This study has not addressed whether the increase of biological production has improved the carrying capacity of the pasturelands or if this is a result of an increase in lower grade species. Increased vegetation cover would nevertheless bind the loose soil and thus decrease soil erosion potential. The coarse resolution of the data set makes it difficult to evaluate the results, and attempts to illuminate underlying causes of the trends must be regarded as speculative. But the spatial pattern of increasing/decreasing NDVI presented in this study is nonetheless interesting and confirms results presented in other recent research addressing reclamation and improvement for different parts of the Mu Us region on the Ordos pastures (26, 27). Much manpower and money have been spent on improving the vegetation cover on the Ordos Plateau over the last decades, and it could be a combination of these measures that is resulting in the positive biomass trends registered by the sensors aboard the NOAA satellites. The verification of these results requires the combination of a high-resolution data set and NPP models applied over a longer time period. Whether northern China is winning the battle against desertification is an issue to be addressed in future research.

References and Notes

1. Longworth, J.W. and Williamson, G.J. 1993. *China's Pastoral Region*. CAB International. Wallingford.
2. Leng, S. 1994. Human impacts on environmental degradation of the Ordos. *J. Arid Land Resources Environ. 8*, 44–52. (In Chinese, abstract in English).
3. Zhu, Z. and Wang, T. 1993. Trends of desertification and its rehabilitation in China. *Desertification Control Bull. 22*, 27–30.
4. Brown, L. 1995. *Who Will Feed China: Wake-Up Call for a Small Planet*. Earthscan Publications Ltd. London, 160 pp.
5. Sun, X. and Yu, Z. 1996. Grassland degradation in the main pastoral provinces of China. *Chinese J. Arid Land Res. 8*, 281–285.
6. Zheng, D. 1994. Desertification and its Management in China. *Chinese J. Arid Land Res. 7*, 81–95.
7. Waldron, A. 1990. *The Great Wall of China*. Cambridge University Press. Cambridge, UK.
8. Zhu, Z., Liu, S., Wu, Z. and Di, X. 1986. *Deserts in China*. Institute of Desert Research. Academia Sinica. Lanzhou. 132 pp.
9. Luk, S.H. 1983. Recent trends of desertification in the Maowusu desert, China. *Environ. Conserv. 10*, 213–223.
10. Statistical Yearbook of Inner Mongolia 1997. Hohot, P.R. China.
11. *Grassland and Grassland Sciences in Northern China*. 1992. National Research Council. National Academy Press. Washington, USA. 214 pp.
12. Defries, R.S. and Townsend, J.R.G. 1994. NDVI-derived land cover classifications at a global scale. *Int. J. Remote Sens. 15*, 3567–3586.
13. Derrien, M., Farki, B., Legléau, H. and Sairouni, A. 1992. Vegetation cover mapping over France using NOAA-11/AVHRR. *Int. J. Remote Sens. 13*, 1787–1795.
14. Maselli, F., Conese, C., Petkov, L. and Gilabert, M. 1992. Use of NOAA-AVHRR NDVI data for environmental monitoring and crop forecasting in the Sahel. Preliminary results. *Int. J. Remote Sens. 13*, 2743–2749.
15. Ehrlich, D., Estes, J.E. and Singh, A. 1994. Applications of NOAA-AVHRR 1km data for environmental monitoring. *Int. J. Remote Sens. 15*, 145–161.
16. Eklundh, L.R. 1996. *AVHRR NDVI for Monitoring and Mapping of Vegetation and Drought in East African Environments*. Chartwell-Bratt Ltd, Kent, UK. 187 pp.
17. Tucker, C.J., Newcomb, W.W. and Dregne, H.E. 1994. AVHRR data sets for determination of desert spatial extent. *Int. J. Remote Sens. 15*, 3547–3565.
18. James, M.E. and Kalluri, S.N.V. 1994. The Pathfinder AVHRR land data set: An improved coarse resolution data set for terrestrial monitoring. *Int. J. Remote Sens. 15*, 3347–3363.
19. Myneni, R.B., Keeling, C.D., Tucker, C.J., Asrar, G. and Nemani, R.R. 1997. Increased plant growth in the northern high latitudes from 1981 to 1991. *Nature 386*, 698–702.
20. Purevdorj, Ts., Tateishi, R., Ishiyama, T. and Honda, Y. 1998. Relationships between percent vegetation cover and vegetation indices. *Int. J. Remote Sens. 19*, 3519–3535.
21. Zhang, K. and Zhao, K. 1989. Afforestation for sand fixation in China. *J. Arid Environ. 16*, 3–10.
22. Smil, V. 1993. *China's Environmental Crises*. M.E. Sharpe, Inc. New York, 257 pp.
23. Walls, J. (ed.). 1982. *Combating Desertification in China*. UNEP Reports and Proceedings Series 3.
24. Li, C., Koskela, J. and Luukkanen, O. 1999. Protective forest systems in China: Current status, problems and perspectives. *Ambio 28*, 341–345.
25. Ho, P. 1998. Ownership and control in Chinese rangeland management since Mao. In: *Cooperative and Collective in China's Rural Development*. Vermeer, E.B., Pieke, F. N. and Chong, W.L. (eds). M.E. Sharpe, Inc. New York. pp 196–235.
26. Wu, W., Wang, X. and Yao, F. 1997. Applying remote sensing data for desertification monitoring in the Mu Us Sandy Land. *J. Desert Res. 17*, 415–420. (In Chinese, abstract in English).
27. Fullen, M.A. and Mitchell, D.J. 1994. Desertification and reclamation in north-central China. *Ambio 23*, 131–135.

28. Acknowledgement. This study has been a part of an international project cooperation entitled: *Land Cover Conversion, Land Degradation and Desertification in North China.—An Assessment of Change* initiated and coordinated by the Remote Sensing and GIS Laboratory, University of Lund, Sweden, and I would like to thank the Swedish National Space Board and the Crafoord Foundation for its generous economic support to this project. I would also like to thank the Institute of Remote Sensing Applications (IRSA) in Beijing and the Institute of Desert Research in Lanzhou, Chinese Academy of Sciences, for the help and support in fieldwork. I would additionally like to thank SSAG and Hierta Retzius Fond for the economic support that has made fieldwork possible.
29. Data used in this study include data produced through funding from the Earth Observing System Pathfinder Program of NASA's Mission to Planet Earth in cooperation with National Oceanic and Atmospheric Administration. The data were provided by the Earth Observing System Data and Information System (EOSDIS), Distributed Active Archive Center at Goddard Space Flight Center which archives, manages, and distributes this data set.
30. First submitted 5 August 1999. Accepted for publication after revision 11 April 2000.

Micael Runnström is a PhD student at the Department of Physical Geography, Lund University, Sweden. His thesis focuses on environmental response to human activities and climate during the last 50 years but especially since the change of political systems in 1979. His address: Department of Physical Geography, University of Lund, Sölvegatan 13, SE-221 00 Lund, Sweden. Email: Micael.Runnstrom@Natgeo.lu.se